

## Synthesis of Thin-Film Electrodes Based on LiPON and LiPON–LLTO–LiPON

A. G. Belous<sup>a</sup>, O. I. V'yunov<sup>a, z</sup>, L. L. Kovalenko<sup>a</sup>, O. Bohnke<sup>b</sup>, and C. Bohnke<sup>b</sup>

<sup>a</sup>Vernadskii Institute of General and Inorganic Chemistry, pr. Palladina 32/34, Kiev, 03680 Ukraine

<sup>b</sup>Institut des Molecules at Materiaux du Mans (MVR 6283 CNRS), Cedex 9, Le Mans, 72085 France

Received February 21, 2013

**Abstract**—Thin lithium-conducting amorphous films of lithium phosphorus oxynitride (LiPON) are synthesized by high-frequency (HF) magnetron sputtering. The effect of sputtering conditions (HF power, support temperature, working gas pressure, and deposition time) on the microstructure of LiPON films is studied. The optimal conditions of HF magnetron sputtering that allow dense, uniform, crack-free, air-stable, amorphous thin LiPON films to be formed are studied. The composite solid electrolyte LiPON–LLTO–LiPON is synthesized based on LiPON films and the  $\text{La}_{2/3-x}\text{Li}_x\text{TiO}_3$  (LLTO) ceramics characterized by the high conductivity with respect to lithium ions but unstable in contact with metal lithium. Its microstructure and electrophysical properties are studied. It is found that the LiPON film prevents the chemical reaction of metal lithium with the LLTO solid electrolyte. Due to the high chemical stability and the enhanced conductivity, the composite solid electrolyte based on LiPON–LLTO–LiPON can be used in electrochemical devices.

**Keywords:** LiPON film, high-frequency magnetron sputtering, composite solid electrolyte LiPON–LLTO–LiPON, lithium batteries

**DOI:** 10.1134/S1023193514060020

### INTRODUCTION

Solid lithium rechargeable batteries are of considerable scientific and practical interest. This is explained by several unique properties typical of lithium batteries, particularly, the absence of liquid electrolyte and the wide working temperature range (from  $-20$  to  $+140^\circ\text{C}$ ). They can be made of any shape and size and are safe throughout the whole range of working conditions [1]. The main components of a solid lithium battery are the anode (as a rule, metal lithium) and the cathode ( $\text{LiCoO}_2$ ,  $\text{V}_2\text{O}_5$ , etc.) and also the solid electrolyte which should have high conductivity with respect to lithium ions and be stable in contact with the metal lithium anode.

To date, the LiPON ( $\text{Li}_3\text{PO}_4-x\text{N}_y$ ) film synthesized by high-frequency (HF) magnetron sputtering [2] is the promising electrolyte for solid-state lithium batteries. Films LiPON are stable in contact with metal lithium but at room temperature their conductivity with respect to lithium ions  $\sigma$  varies from  $10^{-6}$  to  $10^{-7} \Omega^{-1} \text{cm}^{-1}$  [2].

The electric properties and the microstructure of a thin LiPON film depend on the sputtering conditions: HF power, support temperature, working gas pressure, and sputtering time. It should be noted that in the studies found in the literature often dealt with the

effect of only one of sputtering conditions on the properties of LiPON films. For example, it was shown that the conductivity of LiPON films increases with the decrease in the nitrogen pressure [3]. This was explained by the fact that the decrease in the nitrogen pressure during sputtering induces an increase in the concentration of triply coordinated nitrogen atoms  $-\text{N}<$  (conditionally designated as Nt) as compared with doubly coordinated nitrogen atoms  $-\text{N}=\text{}$  (conditionally designated as Nd) in the LiPON film. Moreover, the conductivity increased with the increase in the ratio (Nt)/(Nd). The information on the effect of the HF sputtering power on the conductivity of LiPON films is controversial. On the one hand, the conductivity was observed [4, 5] to increase with the decrease in the sputtering power. On the other hand, a decrease in the conductivity with the decrease in the HF sputtering power was observed [6]. An increase in the temperature at the LiPON film deposition induced an increase in the conductivity [7]. This was explained by the fact that the rise in the temperature during the deposition induces an increase in the concentration of both total nitrogen and its triply coordinated form  $-\text{N}<$ . Simultaneously, the amount of bridge oxygen decreases. It was also shown that the conductivity of the LiPON film increases with the increase in the nitrogen flow rate to reach the maximum at  $3 \times 10^{-6} \Omega^{-1} \text{cm}^{-1}$  [8]. At the same time, the total effect of changes in the conditions of HF sputter-

<sup>z</sup> Corresponding author: vyunov@ionc.kiev.ua (O.I. V'yunov).

ing (HF power, support temperature, working gas pressure, and sputtering time) on the formation of the LiPON film microstructure was never considered.

To enhance the technological parameters of solid-state lithium batteries, it is expedient to make electrolytes of materials with the highest lithium-ion conductivity. To date, the materials with the defective perovskite structure  $\text{La}_{2/3-x}\text{Li}_{3x}\text{TiO}_3$  (LLTO) are known to exhibit the conductivity with respect to lithium ions ( $\sigma \approx 10^{-3} \Omega^{-1} \text{ cm}^{-1}$ ) considerably higher as compared with LiPON [9]. However, they are instable in contact with metal lithium [10]. Hence, it is expedient to elucidate whether it is possible to obtain an electrolyte of LLTO with the high conductivity with respect to lithium and a thin LiPON film placed between the lithium anode and the LLTO electrolyte in order to prevent the interaction between the LLTO electrolyte and the metal lithium anode. The literature contains information on the composite structures built of the LiPON film and the LLTO electrolyte [11]. In the latter study, the LLTO electrolyte was synthesized in the form of films with the islet structure. Additional sputtering of LiPON onto the LLTO film made it possible to obtain the LiPON–LLTf–LiPON polylayer structure which contained no open nonsputtered regions. However, according to the authors, it was difficult to control the chemical composition of the resulting LiPON–LLTf–LiPON system and, hence, interpret the data on conductivity. The authors assumed that the poly-layer structure LiPON–LLTf–LiPON is promising as the electrolyte for separating the anode and the cathode. Furthermore, this composite system LiPON–LLTf–LiPON is the more promising electrolyte as compared with LLTO because prevents the possible chemical interaction of LLTO not only with the metal lithium anode but also with the cathode material (e.g.,  $\text{LiNiO}_2$ ,  $\text{LiCoO}_2$ ) [12]. The latter obstacle additionally limits the use of LLTO as the electrolyte in solid-state lithium devices.

The present study was aimed at investigating the effect of HF magnetron sputtering conditions (HF power, support temperature, sputtering time, working gas pressure) on the microstructure and electrophysical properties of LiPON films and also at studying the microstructure, electrophysical properties, and chemical stability of the LiPON–LLTO–LiPON composite system in contact with metal lithium.

## EXPERIMENTAL

To synthesize LiPON films by HF magnetron sputtering, we used targets of lithium orthophosphate  $\text{Li}_3\text{PO}_4$  synthesized by neutralization of orthophosphoric acid by an excess of lithium hydroxide solution (all chemicals were of the reagent grade). The resulting deposit was dried at  $150^\circ\text{C}$  for 5 h and then annealed

at  $650^\circ\text{C}$  for 2 h. After homogenizing grinding, the samples were pressed and sintered in air atmosphere at  $850^\circ\text{C}$  for 2 h. The LiPON film was sputtered by means of a setup for HF magnetron sputtering based on VUP-5M which was additionally modified in order to control the main technological parameters (magnetron power, support temperature, working gas pressure in the chamber, sputtering time) in wide ranges. The sputtering was carried out in the nitrogen atmosphere [2] onto various supports, namely, *n*-Si (for XRD and IR), polikor  $\alpha\text{-Al}_2\text{O}_3$  (for synthesizing LiPON films at high temperatures), LLTO (for obtaining the composite solid electrolyte). For sputtering of Pt electrodes, the Sputter Coater SC7620 setup was used.

The LLTO supports were synthesized by the solid-state method. As the starting reagents, oxides  $\text{Li}_2\text{CO}_3$ ,  $\text{La}_2\text{O}_3$ , and  $\text{TiO}_2$  (rutile) of the special purity grade were used. The procedure of synthesis is described in detail in [13, 14]. The synthesized supports were polished on an engineering tool Triefus surfex 83201 by gradually decreasing the size of polishing particles down to  $1 \mu\text{m}$ .

The structure and the phase composition of the  $\text{Li}_3\text{PO}_4$  target and LiPON films were studied by the XRD method (diffractometer DRON-4-07,  $\text{CuK}\alpha$  irradiation). Fourier transform IR spectroscopic (FTIR) studies were carried out by means of a Bruker IFS 66 spectrometer with a DTGS detector. The spectra were recorded in the spectrum range of  $400\text{--}4000 \text{ cm}^{-1}$  with resolution of  $2 \text{ cm}^{-1}$ . The film thickness was determined by means of a profilometer Veeco, Deklak 8, Stylus Profilometer; their microstructure was studied by means of a JEOL JSM-6510 microscope, and the distribution and ratio of elements were determined by the energy dispersive analysis (EDX). The interaction of samples with metal lithium electrodes was studied in a glove box with argon atmosphere. Potentiometric studies were carried out by means of a Bio-Logic SA Model VSP, the impedance measurements in the range from 1 MHz to 1 Hz were accomplished by means of a 1260A Impedance/Gain-Phase Analyzer (Solartron Analytical). The equivalent circuit and its components were determined by means of a computer program ZView.

## RESULTS AND DISCUSSION

Figure 1a (curve 1) shows the diffraction pattern of the original ceramic target  $\text{Li}_3\text{PO}_4$ . The results of XRD analysis pointed to the presence of the orthorhombic high-temperature  $\gamma\text{-Li}_3\text{PO}_4$  modification (space group Pmnb;  $a = 0.6114 \text{ nm}$ ,  $b = 1.047 \text{ nm}$ ,  $c = 0.4922 \text{ nm}$  [15]). Figure 1a (curve 2) shows the diffraction pattern of a LiPON film sputtered on *n*-Si. The sample demonstrated no diffraction maximums typical of crystalline phases. The wide peak in the range  $2\Theta = 15^\circ\text{--}35^\circ$

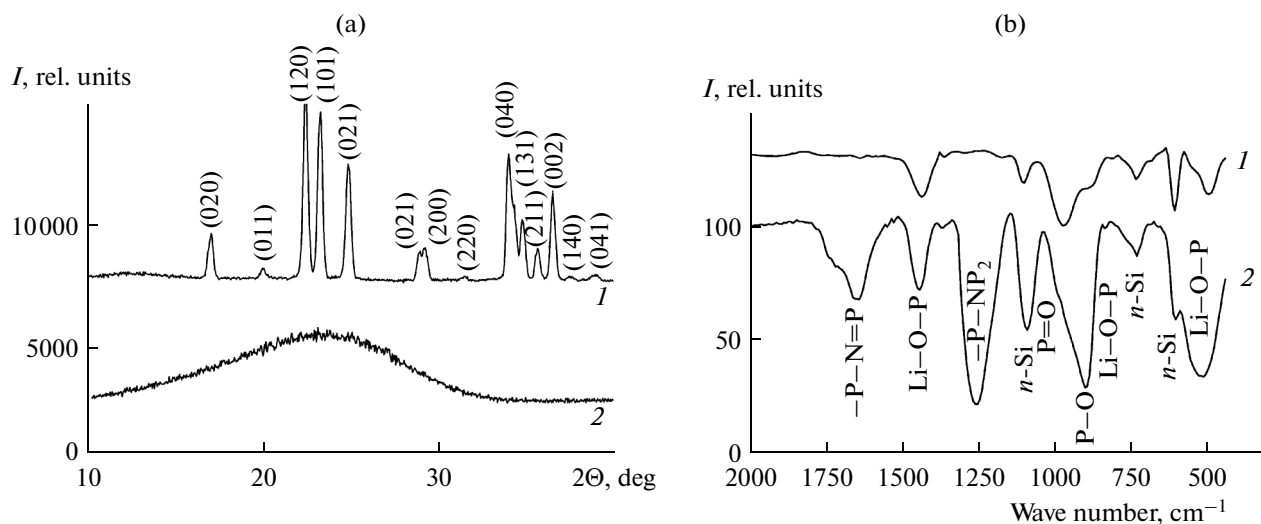


**Fig. 1** (a) Diffraction patterns of (1) Li<sub>3</sub>PO<sub>4</sub> target, (2) LiPON film of the *n*-Si support. (b) IR spectra of (1) Li<sub>3</sub>PO<sub>4</sub> films, (2) LiPON film on the *n*-Si support.

pointed to the amorphous nature of the film, as described in [16, 17]. Figure 1b shows the IR spectra of Li<sub>3</sub>PO<sub>4</sub> and LiPON films deposited on *n*-Si. The IR spectrum of Li<sub>3</sub>PO<sub>4</sub> film supported by *n*-Si (Fig. 1b, curve 1) contained peaks of both the support and the sputtered film. They were assigned to the following groups: Li–O–D (450–585 cm<sup>-1</sup>, 850–925 cm<sup>-1</sup>, 1450–1500 cm<sup>-1</sup> [18]), P=O (1000–940 cm<sup>-1</sup>), P–O (915–880 cm<sup>-1</sup> [18, 19]). In IR spectra of the LiPON film, the intensities of bands belonging to phosphate groups and Li–O–P groups (850–925 cm<sup>-1</sup>) changed (see Fig. 1b, curve 2). The IR spectrum of LiPON films demonstrated new peaks in the ranges of 1300–1250 cm<sup>-1</sup> and 1680–1600 cm<sup>-1</sup>. These peaks were assigned to the following groups: –P–N=P (1680–1610 cm<sup>-1</sup>), –P–NP<sub>2</sub> (1300–1250 cm<sup>-1</sup>) [20–22].

The LiPON films were also deposited on  $\alpha$ -Al<sub>2</sub>O<sub>3</sub> supports by using the HF sputtering power of 2.2 W cm<sup>-2</sup> for 2 h under the nitrogen pressure of 13 Pa. Figures 2a–2c demonstrate microimages of LiPON films deposited on  $\alpha$ -Al<sub>2</sub>O<sub>3</sub> supports without heating and at temperatures of 200°C and 400°C, respectively. Figures 2a'–2b' show the ratios of the main elements: oxygen (in both the film and the support), phosphorus (in the film), and aluminum (in the support), acquired by the energy-dispersive X-ray spectroscopy EDX. It is evident that the film prepared without heating, the support (Fig. 2a) has a relatively dense structure. For the support temperature of 200°C, the film had the islet structure (Fig. 2b). The further increase in the temperature to 400°C was accompanied by the growth of islets formed (Fig. 2c). According to the EDX data, the film synthesized without heating of the support (Fig. 2a') contained the maximum amount of phosphorus. At the support tem-

perature of 200°C, the amount of phosphorus in the film decreased (Fig. 2b'). The decrease in the total content of phosphorus was also observed with the further increase in the support temperature up to 400°C (Fig. 2c'). According to reference data [2, 4, 5, 22], the oxygen-to-phosphorus ratio O/P in the LiPON film structure in the range of maximum conductivity (about 10<sup>-6</sup> Ω<sup>-1</sup> cm<sup>-1</sup>) can vary within 1.77–1.875. According to our experimental data, the O/P ratio varied in the interval of 2–3 with the increase in the support temperature to 400°C. Such a wide interval of variation of the O/P ratio cannot be explained by only the LiPON structural changes. Hence, we assumed that the changes in the film microstructure may be the second factor controlling the O/P ratio.

Based on our studies, it was found that the increase in the support temperature induces the formation of the islet microstructure in the LiPON film.

In the next stage, the films were deposited on supports for 10 h without heating at various HF sputtering powers (0.7, 2.2, and 4.4 W cm<sup>-2</sup>). At the low HF sputtering power (0.7 W cm<sup>-2</sup>), the thickness of the resulting LiPON film was less than 1 μm and the film had the islet structure. For the high HF sputtering power (4.4 W cm<sup>-2</sup>), the resulting film was more than 3 μm thick. This film was unstable in time, and cracked when stored in air. This is explained by the fact that at the high power and, hence, the relatively high sputtering rate, the nitrogen atoms not only displace oxygen in Li<sub>3+y</sub>PO<sub>4-x</sub>N<sub>(y+2x)/3</sub>, but also can be captured in the film in the form of N<sub>2</sub> gas molecules. The exit of the latter during the storage gives rise to cracks [5, 8]. As was shown by our studies, at the HF sputtering power of 2.2 W cm<sup>-2</sup>, the dense, uniform, amorphous

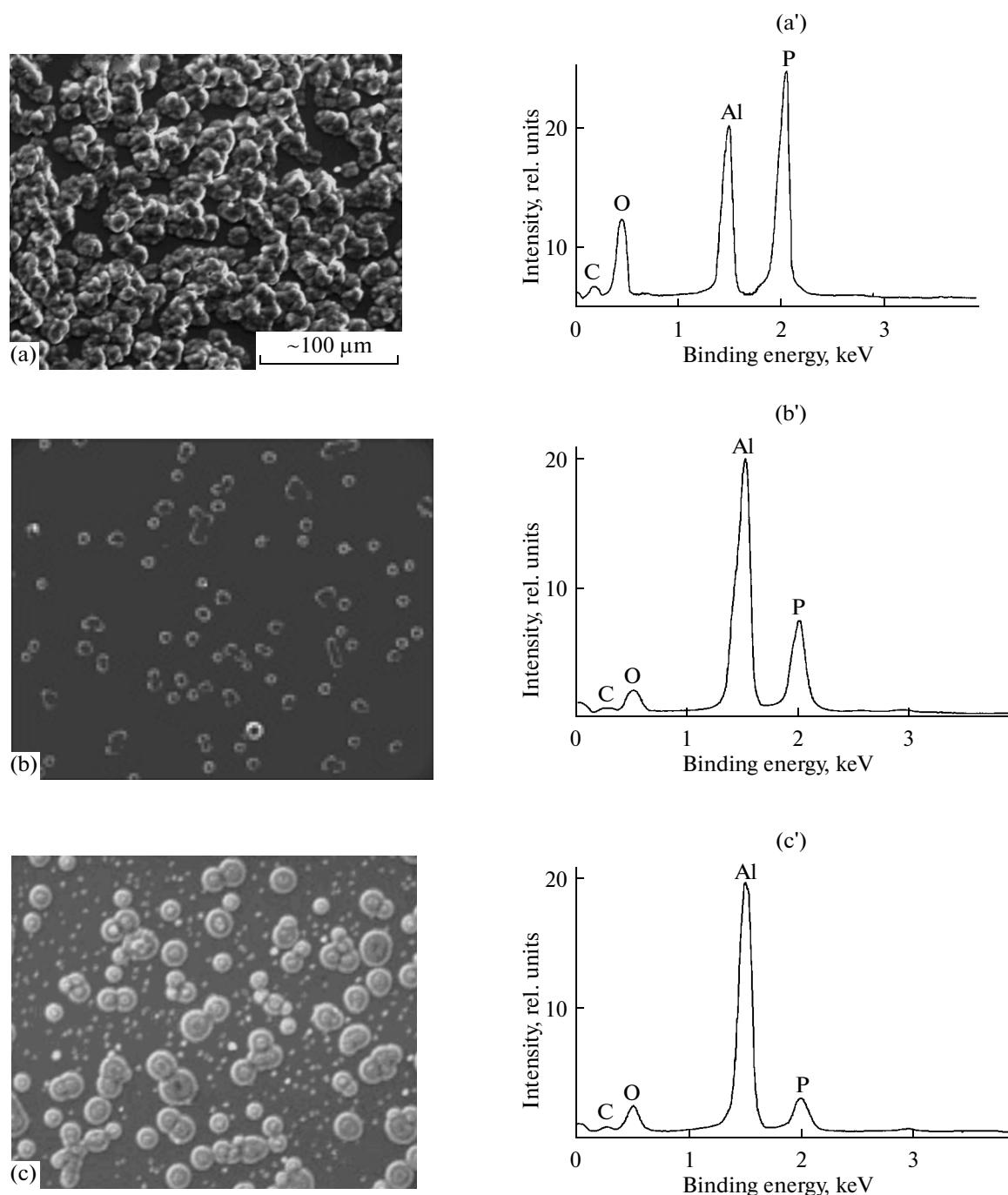


**Fig. 2.** Microimages of LiPON films on  $\alpha$ - $\text{Al}_2\text{O}_3$  supports with different temperatures: (a) without heating, (b) 200°C, (c) 400°C. Distribution of the main elements in  $\alpha$ - $\text{Al}_2\text{O}_3$ -supported LiPON films sputtered at temperatures: (a') without heating, (b') 200°C, (c') 400°C.

films are formed which have no cracks and are stable in air.

To study the effect of nitrogen pressure during sputtering on the LiPON film formation, the films were deposited at the HR power of  $2.2 \text{ W cm}^{-2}$  onto unheated supports at the nitrogen pressure of 1.3 and 13 Pa. In both cases, the sputtering time was 5 and

10 h. For the pressure of 13 Pa, the film thickness increased with time at the constant rate of ca. 5 nm/min. The films had the thickness of 1.5  $\mu\text{m}$  after 5-h sputtering and the thickness of 3.1  $\mu\text{m}$  after 10-h sputtering. After 10-h sputtering, a continuous film with cracks was formed (Fig. 3a). The size of cracks in the LiPON film decreased as the sputtering time

decreased to 5 h (Fig. 3b). At the pressure of 1.3 Pa, the films had the thickness of 1.6  $\mu\text{m}$  after 5-h sputtering and 3.5  $\mu\text{m}$  after 10-h sputtering. The growth rate was 5.3 nm/min, which is close to the previous values. However, the films prepared under these conditions had no cracks after 5-h deposition. At the same time, the thick film (after 10-h sputtering) demonstrated small cracks. Table shows the characteristics of the LiPON film microstructure as a function of conditions of HF magnetron sputtering.

To elucidate the potentials of LiPON films as the protective layer, the film was sputtered on both sides of the preliminarily synthesized and polished ceramic Li-ion conductor, LLTO (the LiPON–LLTO–LiPON system). Due to polishing, the surface of LLTO ceramics acquired intrusions associated with chipped grains. The LiPON film sputtered on the LLTO surface was uniform. During the sputtering, the edges of chipped grains and grooves on the LLTO ceramic surface were “healed”. The analysis of EDX data showed that no decomposition of the LiPON film on the LLTO support occurred during sputtering.

The conductivity of LiPON films prepared by HF magnetron sputtering onto the  $\alpha\text{-Al}_2\text{O}_3$  support was studied by impedance spectroscopy. Figure 4a shows the temperature diagrams of the complex impedance in the Nyquist coordinates for a LiPON film. The additional low-frequency peak in the complex impedance diagrams is associated with the contribution of the capacitance of the near-electrode region. The film conductivity at 20°C was  $3.2 \times 10^{-6} \Omega^{-1} \text{cm}^{-1}$ . Based on the acquired data, the temperature dependence of the conductivity of LiPON films was plotted (Fig. 4b) and the activation energy was calculated to be 0.27 eV. The LiPON film conductivities and activation energies agreed with the literature data [23].

The conductivity of the LiPON film within the polylayer system LiPON–LLTO–LiPON was also determined by the method of complex impedance (Fig. 5a, curve 2). For a comparison, the impedance of LLTO supports without films was also studied (Fig. 5a,

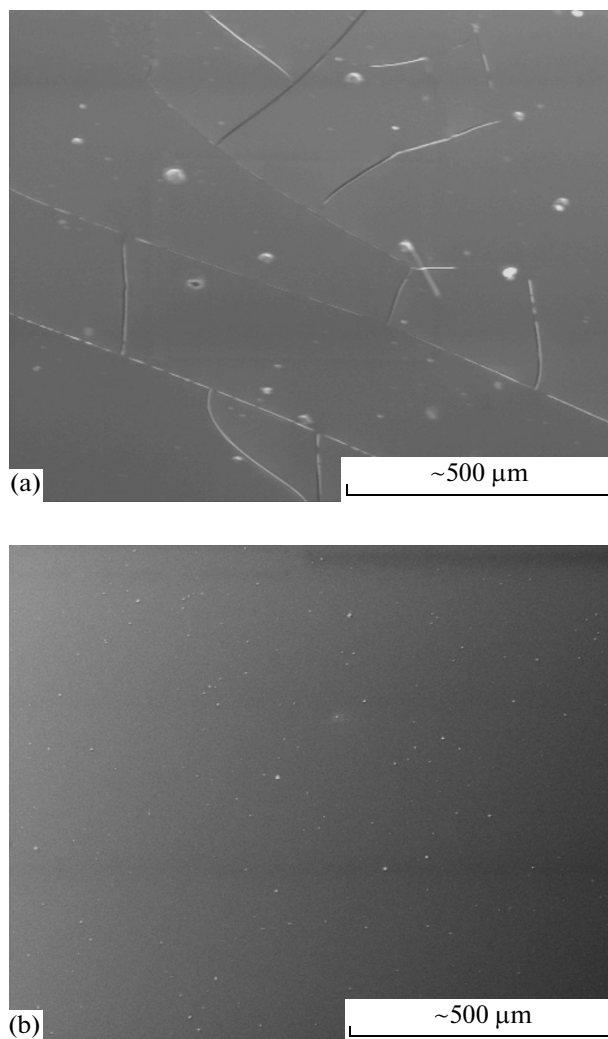


**Fig. 3.** Microimages of LiPON films sputtered onto a glass support without heating at HF sputtering power of  $2.2 \text{ W cm}^{-2}$  and  $\text{N}_2$  pressure of 13 Pa (a) for 10 h and (b) 5 h.

curve 1). According to calculations based on the complex impedance diagram in the Pt–LiPON–LLTO–LiPON–Pt system, the LiPON film conductivity is  $5 \times 10^{-7} \Omega^{-1} \text{cm}^{-1}$ .

Characteristics of the microstructure of LiPON films as a function of conditions of high-frequency magnetron sputtering (HF power  $2.2 \text{ W cm}^{-2}$ , without external heating of the support)

Sputtering conditions		Thickness, $\mu\text{m}$	Cracks	Однородность@	Islet microstructure
nitrogen pressure, Pa	sputtering time, h				
13 Pa	5	1.5	Yes	Yes	Yes
13 Pa	10	3.1	Yes	Yes	No
1.3 Pa	5	1.6	No	Yes	No
1.3 Pa	10	3.5	Small	Yes	Small

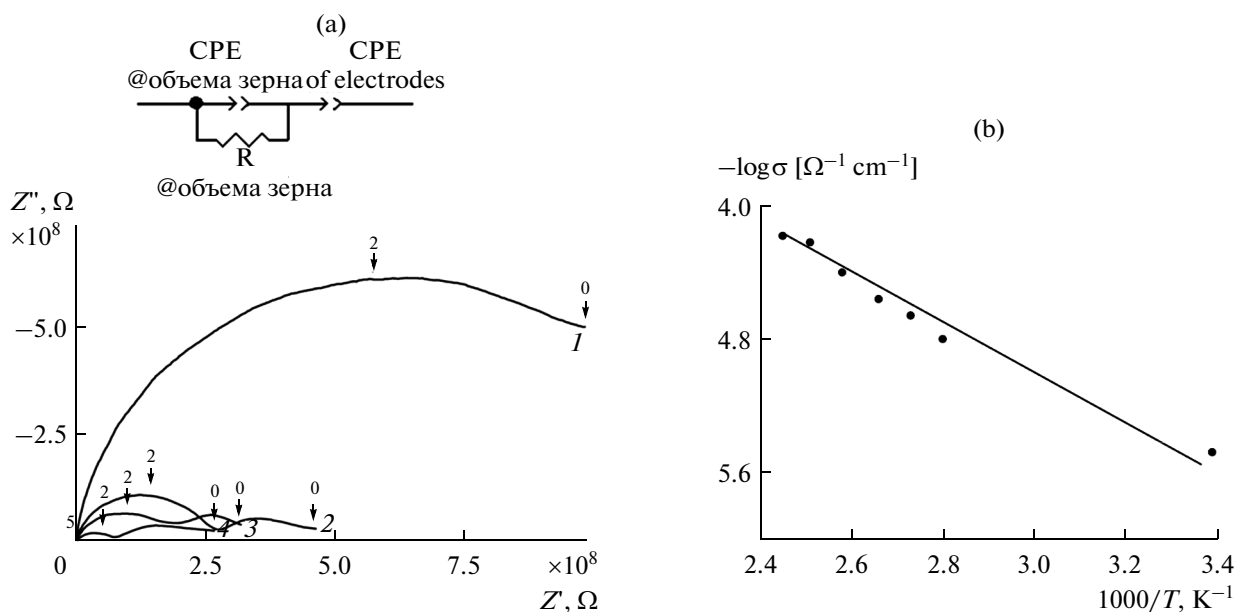


**Fig. 4.** (a) Nyquist plot of complex impedance for a LiPON film at temperatures, °C: (1) 20, (2) 80, (3) 100, (4) 130. Figures at the curves show logarithm of frequency. (b) Temperature dependence of the LiPON film conductivity.

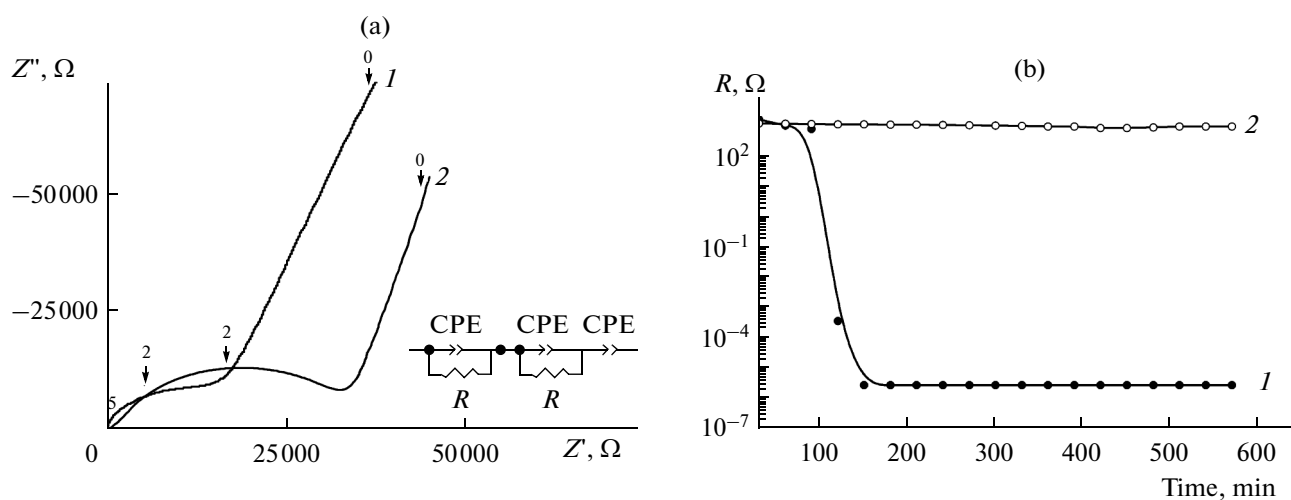


**Fig. 5.** Nyquist plots of the complex impedance of the systems (1) Pt-LLTO-Pt and (2) Pt-LiPON-LLTO-LiPON-Pt. Figures at the curves show logarithm of frequency. (b) Time dependence of the grain volume resistance in systems (1) Li-LLTO-Li and (2) Li-LiPON-LLTO-LiPON-Li.

To elucidate whether the LiPON film protects the LLTO ceramics from the chemical interaction with metal lithium, we studied the electrophysical properties of the Li-LLTO-Li and Li-LiPON-LLTO-LiPON-Li systems.

In the Li-LLTO-Li system, we observed the reaction of metal lithium with LLTO, which was accompanied by a considerable increase in the electron conductivity. This resulted in a considerable decrease in the

resistance of the Li-LLTO-Li sample (Fig. 5b, curve 1) [10]. The electron conductivity increased due to a redox process accompanied by the partial  $\text{Ti}^{4+} \rightarrow \text{Ti}^{3+}$  transition. The presence of  $\text{Ti}^{3+}$  paramagnetic centers induced changes (blackening) in the samples.

In the Li-LiPON-LLTO-LiPON-Li system, the samples were not blackened with time and their resistance remained unchanged for a long time (Fig. 5b, curve 2). The obtained results suggest that the LiPON

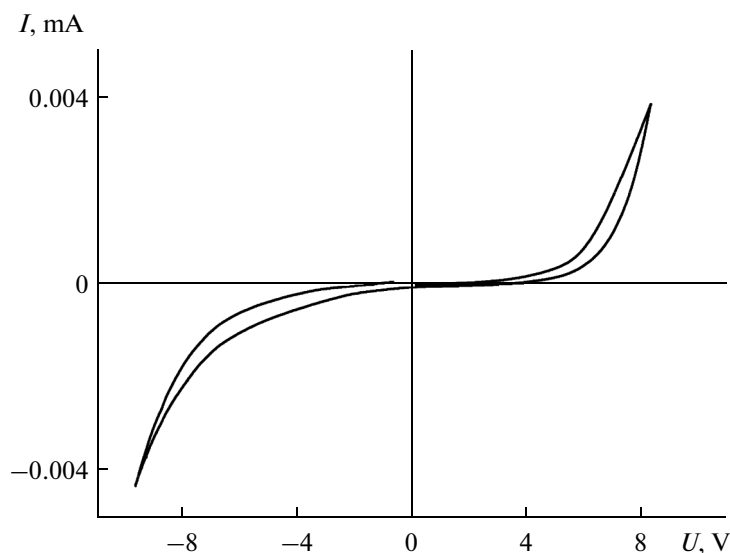


Fig. 6. Cyclic voltammogram in the system Pt–LiPON–LLTO–LiPON–Pt. Potential scan rate 20 mV/s.

film prevents the chemical reaction between the LLTO conductor and metal lithium.

To determine the electrochemical stability of the LiPON film, we carried out potentiodynamic measurements in the Pt–LLTO–Pt and Pt–LiPON–LLTO–LiPON–Pt systems in the potential range of 0–9 V (Fig. 6). The experimental data demonstrated that the Pt–LiPON–LLTO–LiPON–Pt system is electrochemically stable in the range of 0.0–4.5 V.

## CONCLUSIONS

Thus the studies accomplished revealed a relationship between the sputtering conditions and the microstructure, chemical composition, and conductivity of LiPON films synthesized by HF magnetron sputtering. It was shown that the following sputtering conditions (HR sputtering power  $2.2 \text{ W cm}^{-2}$ , deposition rate  $5.3 \text{ nm/min}$ , nitrogen pressure in the working chamber  $13 \text{ Pa}$ , thickness below the critical value (ca.  $3 \mu\text{m}$ ) provide the formation of LiPON films of the high conductivity of  $3.2 \times 10^{-6} \Omega^{-1} \text{ cm}^{-1}$ .

It was found that a LiPON film deposited on the  $\text{La}_{2/3-x}\text{Li}_{3x}\text{TiO}_3$  (LLTO) support by HF magnetron sputtering can form a lithium-conducting protective layer which enhances the chemical stability of the LLTO electrolyte at its contact with metal lithium.

## REFERENCES

1. Va, D. and Mount, J., in *Thin Film Batteries. Vacuum Technology and Coating*, 2007, p. 73.
2. Bates, J.B., Dudney, N.J., Gruzaiski, G.R., Zuhr, R.A., Choudhury, A., Luck, C.F., and Robertson, J.D., *J. Power Sources*, 1993, vol. 43–44, p. 103.
3. Hu, Z., Xie, K., Wie, D., and Ullah, N., *J. Mater. Sci.*, 2011, vol. 46, p. 7588.
4. Hamon, Y., Douard, A., Sabary, F., Marcel, C., Vinacrier, P., Pecquenard, B., and Lenarrer, A., *Solid State Ionics*, 2006, vol. 177, p. 257.
5. Choi, C.H., Cho, W.I., Cho, B.W., Kim, H.S., Yoon, Y.S., and Tak, Y.S., *Electrochem. Solid-State Lett.*, 2002, vol. 5, p. A14.
6. Roh, N.-S., Lee, S.-D., and Kwon, H.-S., *Scr. Mater.*, 2000, vol. 42, p. 43.
7. Jancke, S., Song, J., Dimesso, L., Broetz, J., Becker, D., and Jaegerman, W., *J. Power Sources*, 2011, vol. 196, p. 6911.
8. Fleutot, B., Pecquenard, B., Mrtinez, H., Letellier, M., and Levasscur, A., *Solid State Ionics*, 2011, vol. 186, p. 29.
9. Belous, A.G., Novitskaya, G.N., Polyanetskaya, S.V., and Gornikov, Y.I., *Izv. Akad. Nauk SSSR. Inorg. Mater.*, 1987, vol. 23, no. 3, p. 470.
10. V'yunov, O.I., Gavrilenko, O.N., Kovalenko, L.L., Chernukhin, S.A., Vasilechko, L.O., Kobilyanskaya, S.D., and Belous, A.G., *Russ. J. Inorg. Chem.*, 2011, vol. 56, p. 93.
11. Lee, J., Kim, S., Tak, Y., and Yoon, Y., *J. Power Sources*, 2006, vol. 163, p. 173.
12. Liao, C., Wen, C., and Fung, K., *J. Alloys Compd.*, 2007, vol. 432, p. L22.
13. Belous, A., Yanchevskiy, O., and V'yunov, O., *Chem. Mater.*, 2004, vol. 16, p. 407.
14. Rivera, A., Leo'n, C., Santamari'a, J., Va'rez, A., V'yunov, O., Belous, A., Alonso, J., and Sanz, J., *Chem. Mater.*, 2002, vol. 14, p. 5148.

15. Liu, H.C. and Yen, S.K., *J. Power Sources*, 2006, vol. 159, p. 245.
16. Yu, X., Bates, J.B., Ellison, G.E., and Hart, F.X., *J. Electrochem. Soc.*, 1997, vol. 144, p. 524.
17. Pichonat, T., Lzthien, C., Tiercelin, N., Godey, S., Pichonat, E., Roussel, P., Colmont, M., and Rolland, P.A., *Mater. Chem. Phys.*, 2010, vol. 123, p. 321.
18. Kim, B., Cho, Y.S., Lee, J.G., Joo, K.H., Jung, K.O., Oh, J., Park, B., Sohn, H.J., Kang, T., Cho, J., Park, Y.S., and Oh, J.Y., *J. Power Sources*, 2002, vol. 109, p. 214.
19. Mel'nikova, R.Ya., Pechkovskii, V.V., Dzyuba, E.D., and Malashonok, I.E., *Atlas infrakrasnykh spektrov fosfatov: Kondensirovannye fosfaty* (Atlas of Infrared Spectra of Phosphates. Condensed Phosphates), Moscow: Nauka, 1985.
20. Nyquist, R.A. and Kagel, R.O., *Infrared Spectra of Inorganic Compounds (3800–45 cm<sup>-1</sup>)*, New York: Acad. Press, 1971.
21. Vasilev, A.V., Grinenko, E.V., Schukin, A.O., and Fedulina, T.G., *Infrared Spectroscopy of Organic and Natural Products: the Manual*, S.-Petersburg: State Forest-Technical Acad., 2007.
22. Socrates, G., *Infrared Characteristic Group Frequencies*, Chichester: Wiley, 1980.
23. Kim, Y. and Wadley, H., *J. Power Sources*, 2009, vol. 187, p. 591.
24. West, W.C., Whitacre, J.F., and Lim, J.R., *J. Power Sources*, 2004, vol. 126, p. 134.

*Translated by T. Safonova*

SPELL: 1. ok